International Journal of ChemTech Research
CODEN (USA): IJCRGG ISSN: 0974-4290
Vol.7, No.3, pp 1343-1350, 2014-2015

ICONN 2015 [5th -7th Feb 2015]
International Conference on Nanoscience and Nanotechnology-2015
SRM University, Chennai, India

Ferrite + Polymer nanocomposites for EMI applications

P. Raju, T. Ramesh and S.R.Murthy*

Department of Physics, Osmania University, Hyderabad-500 007, India.

Abstract: Nanosized $Ni_{0.5}Zn_{0.5}Cu_{0.12}Fe_2O_4$was prepared by a microwave hydrothermal method at a low temperature of 160 C/30 min. $Ni_{0.5}Zn_{0.5}Cu_{0.12}Fe_2O_4$/ paraformaldehyde (PFD) composites were prepared by using mechanical milling method. The structure, morphology and ferromagnetic property of ferrite powders and composites were characterized by powder X-ray diffractometer (XRD), transmission electron microscope (TEM), Fourier transform infrared (FTIR) spectra and vibrating sample magnetometer (VSM).It was demonstrated that there was some interaction between the ferrite particles and PFD chains in the nanocomposites. The particle size of the composites varies from 21 nm to 35 nm. The complex permittivity (ε' & ε″) and permeability (μ' & μ″) were measured in the wide frequency range at room temperature. It was observed that the permittivity increased and the permeability decreased with an increase of polymer content. The magnetic properties such as saturation magnetization (M_S) and coercivity (H_C) have been measured and it was found that that the both decreased with the content of polymer. The ferrite+ polymer nano composites were demonstrated as a promising functional material for the absorbing of electromagnetic microwaves. Both the complex permittivity and shielding effectiveness of the ferrite+ polymer nanocomposites increased with the increasing polymer content.
Keywords: Polymer nanocomposites, mechanical milling, complex permittivity, complex permeability, magnetic properties, shielding effectiveness

Introduction

Conducting polymer/ferrite composites with an organizedstructure provide a new functional hybrid betweenorganic and inorganic materials. Polymer onferrite nanoparticles can enhance compatibility with organicingredients, reduce susceptibility to leaching, and avoid aggregation. Thus, composites formed bythe conducting polymer and magnetic ferrites can be usedas EMI shielding materials, and will have good shieldingeffectiveness for various electromagnetic sources. In this connection, ferrite-polymer composites have been a subjected to extensive research[1-3]. Out of all the insulators and conducting polymers, ferrites and polyaniline (PANI) composites were extensively studied[4,5] because of their good environment stability, and relatively easy preparation. Among the different spinel ferrites, NiCuZn ferrites are the most versatile magnetic materials. This is because,NiCuZn ferrites have been widely used to fabricate chip inductors and EMI filters,because of their relatively low sintering temperatureand high resistivity with good performance at highfrequencies.

The electrical and magnetic properties of NiCuZn ferrite+ polymer composites can be tailored by controlling the preparation conditions and amount of polymer filler. At high frequencies, the electromagnetic waves can be effectively shielded by magnetic source and conducting polymer can be effectively shielding the electromagnetic waves generated from the electric source. Thus the composite material having both magnetic and conducting components are used for EMI shielding applications. The traditional methods for the preparation of ferrites involve conventional solid-state synthesis techniques, which are known to have serious limitations, such as chemical inhomogeneity,poor compositional control and the formation of large particles[6]. Several synthesis methods have been developed to prepare ferrite nanoparticles and nanocomposites, including chemical Co-precipitation, hydrothermal processing, sol–gel and mechanical alloying. The last technique, in addition to reduce grain size and mix powders uniformly, has proved to be a powerful tool for the synthesis of various kinds of materials, such as amorphous alloys, nanocrystalline metals and alloys and ceramic materials[7-12]. Hence, in the present investigation NiCuZnferrite (NCZ)/ paraformaldehyde (PFD) nanocomposites have been prepared using mechanical milling method and the effect of the volume fraction of polymer on the frequency dispersion characteristics of the complex permittivity and permeability was studied. The shielding effectiveness (SE) of the nanocomposites was measured and obtained results are presented in this paper.

Experimental method

The nanopowders of $Ni_{0.48}Cu_{0.12}Zn_{0.4}Fe_2O_4$ (NCZ) were synthesized using microwave-hydrothermal method starting with high purity (99.9%) chemicals of nickel nitrate [Ni $(NO_3)_2{\cdot}6H_2O$], zinc nitrate [Zn $(NO_3)_2{\cdot}6H_2O$], copper nitrate [Cu $(NO_3)_2$ $.6H_2O$] and ferric nitrate [Fe $(NO_3)_3{\cdot}9H_2O$] were taken in stoichiometric ratio. These reagents were dissolved in 50 ml of de-ionized water. To this solution, sodium hydroxide (NaOH) was added to maintain the pH of the solution ~12. Controlling of pH is the key factor to synthesize the nano powder. Then the precipitation was transferred into double-walled digestion vessels that have an inner liner and cover made up of Teflon PFA and an outer high strength layer made up of ultempolyetherimide and then treated using M-H method at 160°C/45min. The M-H treatment was performed using a microwave accelerated reaction system (MARS-5, CEM Corp., Mathews, NC). This system uses 2.45GHz microwave frequency and can be operated at 0–100% full power (1200±50 W). The reaction vessel was connected to an optical probe to monitor and control the temperature during synthesis. The product was separated by centrifugation and then washed repeatedly with de-ionized water, followed by drying in an Oven overnight at 60°C. Thus the obtained powders were weighed and the percentage yields were calculated from the total expected based on the solution concentration and volume and the amount that was actually crystallized and a yield of 96% was obtained. Then the as-synthesized powders were characterized by XRD (PhilipsPW-1730 X-ray diffractometer)and TEM (model JEM-2010, JEOL, Tokyo, Japan).

As synthesized nanopowders of $Ni_{0.48}Cu_{0.12}Zn_{0.4}Fe_2O_4$ (NCZ) were mixed with commercially available paraformaldehyde (PFD, Sigma-Aldrich, density is 30.03g/mol) at different weight percentage to obtain the composites of $xNi_{0.48}Cu_{0.12}Zn_{0.4}Fe_2O_4$ + (1-x) paraformaldehyde, ($0 \leq x \leq 1$). The mixed powders were mechanical milled using a RetschCo high energy planetary ball mill by using the hardened tungsten carbide (WC) vial together with ten 12 mm WC balls for 30 hr. A ball to powder mass charge ratio of 14:1 was chosen. The speed of the mill was set at 400 rpm with interval at 40 minutes. The 30-hrs milled powders were subjected to anneal at 110°C/30 min in an air atmosphere. The ball milled powders were pressed into 8 mm pellets and toroidal specimens. The samples were characterized by X-ray diffraction (XRD), scanning electron microscopy (SEM, LEICA, S440i, UK) and fourier transform infrared spectrometer (FTIR, Brucker tensor 27). The magnetic properties such as saturation magnetization (M_s) and coercive field (H_c) for the composites were obtained from the recorded hysteresis loops obtained with the help of Vibrating Sample Magnetometer (VSM, Model DMS 1660 model) at room temperature. The frequency dependence of complex permittivity (ε' & ε'') and complex permeability (μ' & μ'') studies were measured in the frequency range of 1MHz -1.8 GHzusing impedance analyser (Agilent 4291B) at room temperature.

The shielding effectiveness (SE) of the nanocomposites was measured by a Network Analyzer (Agilent E5062A: 30 MHz to1 GHz) using a coaxial transmission line method. The sample was disk-shaped with 120 mmdiameter and 2 mm thickness and contained 6 holes of 4mmdiameter. The shielding effectiveness (SE) is determined as aratio of the power received without shielding material (P_0) to that of the power received with shielding material (P_1): $SE = 10 \log(P_0 / P_1)$.

Results and discussions

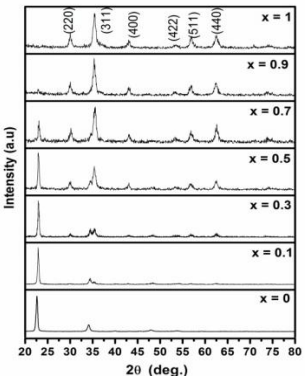

Fig. 1 XRD patterns of xNCZ+(1-x) PFD (x = 0, 0.1, 0.3, 0.5, 0.7, 0.9 and 1) composites.

Fig. 1 shows XRD patterns for thenanocomposites along with NCZ and PFD. The patterns were recorded at room temperature using Cu-Kα radiation(λ=1.5406 Å), in the 2θ range 20° to 80° with step size 0.03° operating at 40 kV and 30mA. The sample x=1 shows clear spinel cubic phase without any impurities. Thetwo XRD peaks at 22° and 34° for x=0 are ascribed to the characteristic peaks of the PFD chains.It is observed from the figure that the degree of crystallinity of the composites increased with annealing for 30h at 110°C/30 min. The intensity of the ferrite peaks are influenced by the addition of polymer. It is found that the intensity of the ferrite peaks decreased with polymer and vice versa. The diffused peaks of the polymer disappeared with ferrite content due to the ferrite nanoparticles interfered with polymer chains. It can also be observed from the XRD that the diffraction peaks were narrow initially for pure ferrite and become broadened with higher additions of polymer. Crystallite size has been calculated using Scherer's equation($D_m = K\lambda/\beta \cos\theta$, K is a constant, λ wavelength of x-rays, β the full width half maximum and θ the diffraction angle), based on the widening of three strongest peaks of a certain phase and presented in the Table 1. It is observed from the table that the crystallite size of the composites is in nanorange and decreased with an increase of polymer. The lattice parameters of composites were calculated with the help of (3 1 1) peak and is presented in Table 1. It is observed that with an increase of PFD the diffraction peak (3 1 1) is shifted towards lower Bragg angle side, which indicates that NCZ particles are bonded to polymer chains and also due to the stress induced by the ferrite particles. The incorporation of polymer into NCZ does not change the crystal structure of the ferrite but the lattice is distorted.

Table 1.Structural, dielectric and magnetic data of NCZ-PFD nanocomposites at room temperature.

NCZ (x%)	lattice constant (3 1 1) plane (a)(Å)	Crystallite size (nm)	X-ray density (g/cm^3)	ε′ ------ at 1MHz--------	ε″	μ' (emu/g)	μ″	M_sH_c (Oe)	
x= 1	8.439	35	5.213	22	2.12	1346	1.88	57	15
x = 0.9	8.423	31	5.196	27	2.24	1288	1.96	45	11
x = 0.7	8.422	28	5.098	29	2.54	1178	2.01	33	8
x = 0.5	8.412	23	4.956	35	2.78	990	2.24	22	6
x = 0.3	8.404	21	4.886	39	2.82	885	2.58	11	5
x= 0.1	8.371	21	4.874	41	2.89	---	---	---	---

Particle size and morphology of NCZ were determined using transmission electron microscopy (TEM). It can be seen from the picture (Fig.2) that the particles are evenly distributed, aggregated and exhibited rounded irregular shapes. The selected-area diffraction (SAD) patterns of these specimens reveal the formation of single-phase ferrite. The diffraction rings, characteristic of nanocrystalline aggregates, have been indexed. Indeed the bright and dark field images reveal nanometric particles with a broad (28–34 nm) size distribution. Occasional spots in the SAD pattern may arise from coarse crystallites or agglomerates. The mean particle sizes obtained from the TEM picture is 32 nm. Thus, the particle sizes calculated from TEM and XRD are almost comparable with each other.

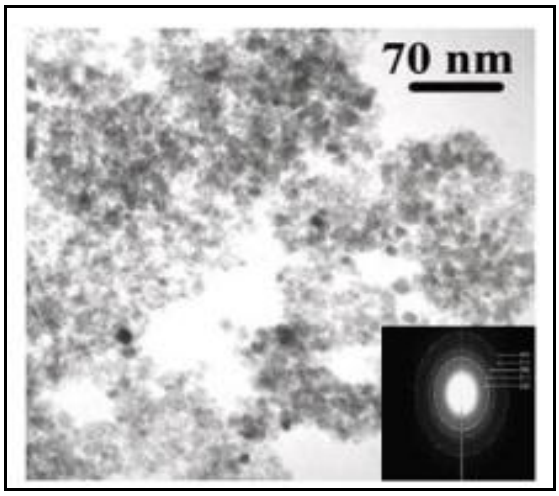

Fig. 2 TEM picture for as synthesized nanopowder of NCZ.

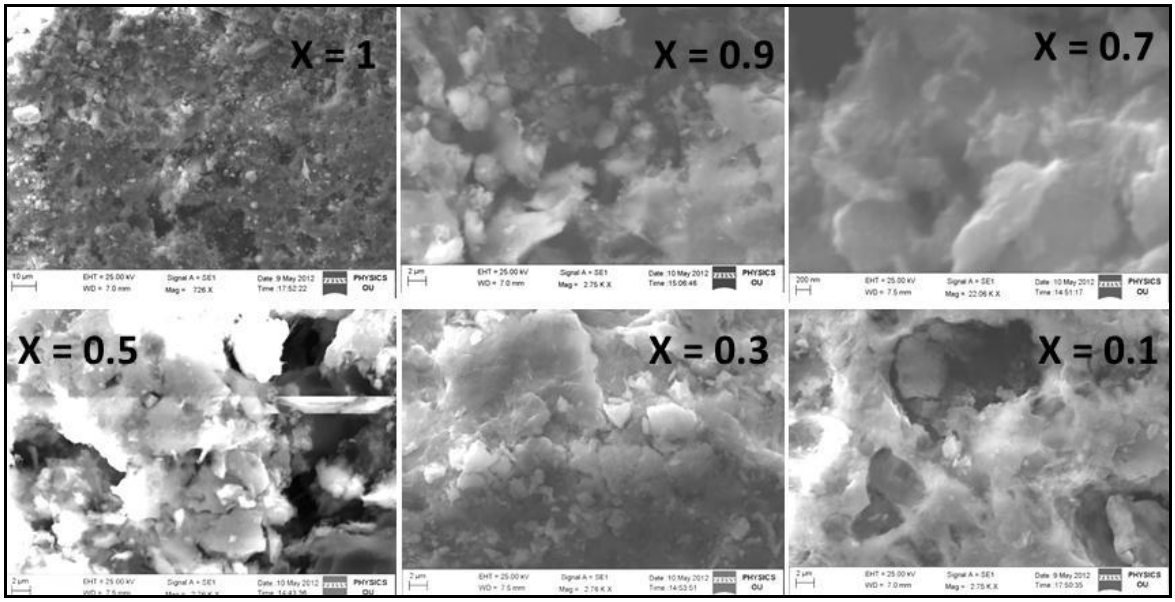

Fig. 3 SEM images of pictures xNCZ+(1-x) PFD (x = 0.1, 0.3, 0.5, 0.7, 0.9 and 1) nanocomposites.

Fig. 3 gives SEM pictures for thex = 0.1, 0.3, 0.5, 0.7, 0.9 and 1. It can be seen from the SEM micrographs that the connectivity of NCZ grains are discontinued due to the presence of polymer, which leads to the variation in the dielectric and magnetic properties of the composites. As x increased the ferrites grains are agglomerated due to the strong interaction between the ferrite particles and this led to the NCZ powders not being uniformly distributed in the PFD matrix. It is also clear that as the x increased the average grain size of the ferrite is also increased. The theoretical density of the composites is calculated from the equation: $\rho = (m_1+m_2) / (m_1\rho_1 + m_2 \rho_2 + \rho_1 \rho_2)$, where m_1 and m_2 are the masses of NCZ and PFD, respectively, ρ_1, ρ_2, and ρ the theoretical densities of NCZ, PFD and composites, respectively. The bulk density of the composites is in the range of 95%–96% of the theoretical density. The theoretical density of the nanocomposites decreased with polymer content since the molecular weight of ferrite is more than that of the polymer. The average porosity is 6% in the present nanocomposites.

The FT-IR spectra of the nanocomposites are shown in Fig. 4. It can be seen from the figure that the peaks observed at 3430 $cm^{-1}$and 2960 cm^{-1} are ascribed to the hydroxyl stretching and C–H stretching vibrations, respectively. The peaks observed at 1250 cm^{-1} and 1110 cm^{-1} are associated with the C–O–C symmetrical stretching vibration, and the peaks at 949 cm^{-1} and 841 cm^{-1}correspond to the C–H bending wagging vibration and the deformation vibration of O– C–O of PFD[13,14]. In addition, the absorption peaks at 609 cm^{-1} and 409 cm^{-1} observed are due to the intrinsic vibration of the tetrahedral and octahedral sites in the NCZ ferrite particles. It can be seen from the vibration spectra of spinel ferrite a high frequency band υ_1 (600–580 cm^{-1}) and the low-frequency band υ_2(440–400 cm^{-1}) has been observed. These bands are attributed to the

intrinsic vibration of the tetrahedral sites and the octahedral sites, respectively[15]. These results indicate that the NCZ nanoparticles are well dispersed in the PFD matrix.

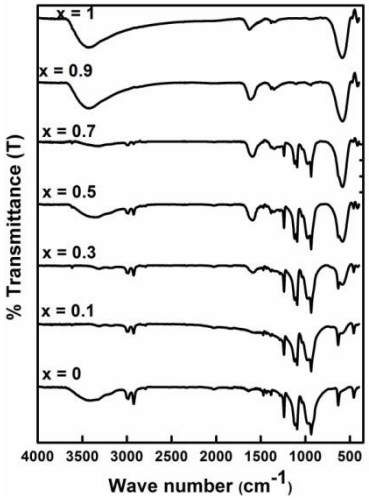

Fig. 4 FTIR spectra for NCZ, PFD samples and nanocomposites.

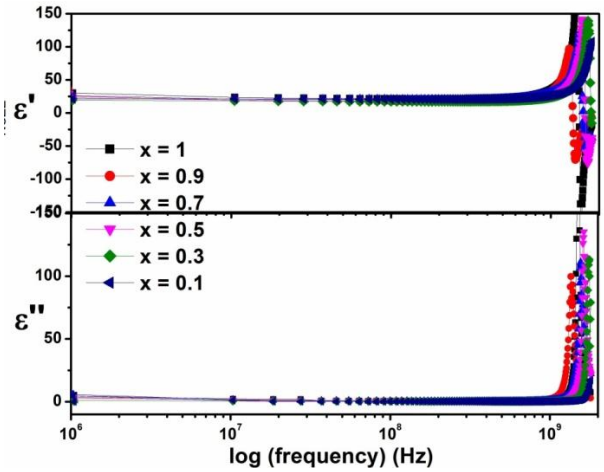

Fig. 5 Frequency dependence of real (ε') and imaginary (ε″) part of permittivity of xNCZ+(1-x) PFD (x = 0.1, 0.3, 0.5, 0.7, 0.9 and 1) nanocomposites.

Fig 5 shows the frequency variation of real (ε′) and imaginary (ε″) parts of permittivity for the composites under investigation was measured in the range of 1MHz to 1.8 GHz. It can be seen from the figures that the value of ε′ remains constant upto a frequency 400 MHz and increases further increase of frequency. It is observed that with polymer content, the dielectric constant increased for composite samples. In PFD polymer, strong polarization occurs due to the presence of polaron/bipolaron and other bound charges which leads to high values of ε′ and ε″. The variation of ε″ with frequency may be explained similar to that of ε′ variation with frequency.It can be seen from the figure that the value of ε″ is small and remains almost constant from 1 MHz to 400 MHz. Whereas with the increase of frequency, the ε″ increased above400 MHz may be due to the following of hopping electrons with the external field. When the hoping frequency of the electrons is equal to that of the external applied electric field, a peak is obtained and it is called as the dielectric resonance. In the present composites, resonance peak is observed above 1GHz. It is observed that with ferrite, the values of ε″ increased. The increase of dielectric loss with ferrite volume concentration may be explained as follows: each composite consists of a ferrite particle surrounded by a layer of polymer, although there can be distributions in the layer thickness. As the ferrite content increases with a corresponding decrease in the polymer ratio, the homogeneity of the composites decreases because the composite now consists of, in addition to the composite particles, some ferrite particles which are not covered by the polymer (due to a reduction in the polymer content), thus leading to a heterogeneous mixture. With increase in the ferrite content, therefore, this heterogeneity increases which results in an increase in loss.

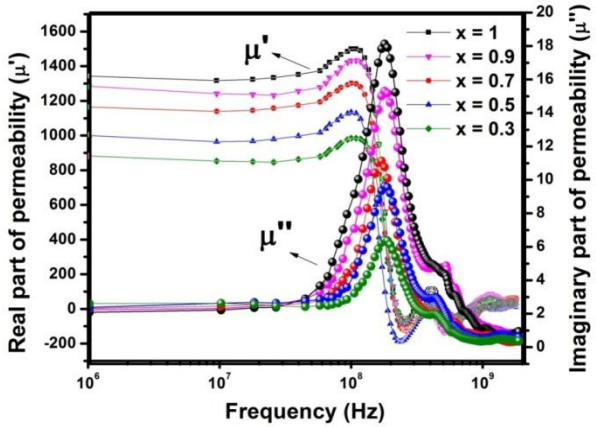

Fig. 6 Frequency dependence of complex permeability (μ' & μ'') of xNCZ+(1-x) PFD (x = 0.3, 0.5, 0.7, 0.9 and 1) nanocomposites.

Fig. 6 gives the complex permeability (μ' & μ") spectra forNCZ-PFD nanocomposites. It can be seen from fig 6a that the value of μ′ remained almost constant, until the frequency was raised to a certain value and then began to decrease at higher frequency. The imaginary (μ′′) part of permeability gradually increased with the frequency and took a maximum at a certain frequency, where the μ′ rapidly decreases. This feature is well known as natural resonance. It can be seen from the figure that the value of real part of permeability (μ') is decreased with an increase of polymer content in the composite. The value of real part of permeability (μ′) for all the samples under investigation remains constant with an increase of frequency from 1MHz to 110 MHz. In composite materials, the decrease of μ′ is may be due to the decrease in the interaction between ferrite particles since in the composite ferrite particles are surrounded by the nonmagnetic polymer layers which discontinuous the magnetic flux in the material. This would result in the decrease of permeability of the composite. The magnetic loss in the composites and pure ferrite are caused by sum of domain wall resonance and natural resonance at high frequencies. Therefore, with ferrite content, the magnetic loss increased.

Resonance in ferrites arises due to coupling of the energy when the precessional frequency of the electron spins is the same as that of the microwave frequency. The frequency at which the resonance peak occurs is decided by the low frequency permeability of the ferrite, according to Snoek's rule[16] and that $\mu'.f_r$ = constant; where $f_r$is the resonance frequency. This equation implies that higher the μ′ values lower the frequency at which resonance would occur. With a decrease in the ferrite content in the composites, μ′ is expected to decrease with the resonance frequency shifting correspondingly to higher frequencies. The collapse of the magnetic connectivity between the ferrite particles gives rise to shape anisotropy, which introduces demagnetizing fields[17]. With increase in the polymer content the demagnetizing fields would increase resulting in higher resonance frequency[17].

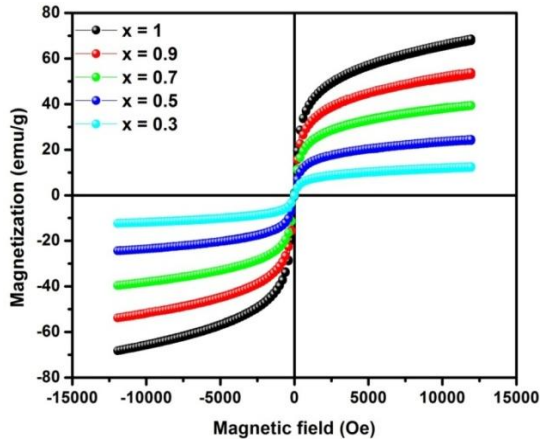

Fig. 7 Magnetization loops of xNCZ+(1-x) PFD (x = 0.3, 0.5, 0.7, 0.9 and 1) nanocomposites.

Fig. 7 shows the hysteresis loops of the pure ferrite and nanocomposites, expect for the sample NCZP5. From the hysteresis loops the values of M_S and H_C for ferrite and composites are obtained and the results are presented in the Table 1. It can be seen from the table that the saturation magnetization (M_S) for x = 1 is 57emu/g at 300K, and decreased with an increase of polymer content. In all composites, a notably small value of coercive force is observed with negligible retentivity, which indicates the ferrimagnetic nature of the material[9, 18]. According to the equation $M_S = \varphi m_S$, $M_S$is related to the volume fraction of the magnetic particles(φ) and the saturation moment (m_s) of a single particle[19]. Besides, a nonmagnetic PFD plays a part in isolating the magnetic particles, which results in the transformation of the collinear ferromagnetic order of ferrite into a noncolinear arrangement and disruption of ferromagnetic order[20]. As PFD content increases, the demagnetic effect is notable. Therefore, the saturation magnetization of NCZ-PFD composites is less than that of pure structures and depends on particle size, particle shape, magnetic anisotropy, etc. During annealing of composites, the polymer PFD is absorbed on the surface of ferrite particles and in between ferrite particles acts as grain boundaries which may create defects, pores and cracks, etc which leads to the decrease of magnetocrystalline anisotropy and thus by decreases the coercivity.

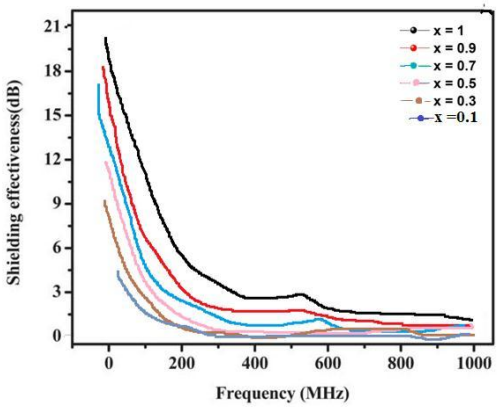

Fig. 8 Shielding effectiveness in xNCZ+(1-x) PFD (x = 0.1, 0.3, 0.5, 0.7, 0.9 and 1) nanocomposites.

Fig. 8 gives the shielding effectiveness (SE) of all the nanocomposites.It can be seen from the figure that the value of SE increased with the increasing polymer content in the nanocomposites. In general, the material can be accepted for the shielding purpose if the SE is higher than 5 dB and 15 dB, in the low frequency range[21]. The present ferrite-polymernanocomposites possess acceptable shielding effectiveness (~5 dBto20 dB) in the low frequency range of 50 MHz to 150 MHz for the sample 3 (60%). It is evident from the figure that the shielding effectiveness of the nanocomposites decreased with an increase in frequency and this is due to the ferrite-on-polymer nanocomposites may onlybe effective for the electromagnetic interference shielding at low frequencies. In the polymer, the electromagnetic wave was reduced due to the intrinsic dipole polarization. But for ferrites, the attenuation of electromagnetic microwaves is due to the existence of free electrons and material defects. The good transmittance of electromagnetic microwaves on the inside of the composites was observed due to evenly dispersed ferrite particles on thesurface of polymer and resulting in larger attenuation of the electromagnetic wave. Thus this type of the ferrite-on-polymer nanocomposites possess potential application sat low frequency, which in turn used in the industrial robots or medical apparatus from the electromagnetic interference, and especially keep the human body from radiation.

Conclusions

A NCZ-PFD nanocomposite was successfully prepared using the mechanical-milling process. With thePFD content, the permittivity of the all composites increased and permeability decreased. The real part of permittivity and permeability of all the composites have shown good frequency stability. It is also observed that the present composites shows a low dielectric and magnetic losses within the measurement range. Such magnetic composites are candidates for the capacitor-inductor integrating devices such as electromagnetic interference filters in RF communications. The applicability of the nanocomposites for electromagnetic microwave absorption wastested in terms of their dielectric loss properties and shielding effectiveness. It was found that the permittivity and shielding effectiveness of the present nanocomposites increased with increase in polymer content. The present nanocomposites possess high permittivity losses for the sample when compared to other magneticshielding composites.

The nanocomposites also exhibited a good match of real and imaginary parts of the complex permittivity in the frequency range (1 MHz to 1 GHz). This superior property allows us to say that the present nanocomposites to function within an extended absorbing band.

Acknowledgements

The authors are thankful to UGC-BSR,New Delhi, India for providing financial assistance.

References

1. T. Mäkelä, S. Pienimaa, T. Taka, S. Jussila,H. Isotalo, Synth.Met. 85 (1997)1335-1336.
2. S. Kuwabata, S. Masui,H. Yoneyama, Electrochim.Acta.44[8] (1999)4593-4600.
3. J. Q. Kan, X. H. Pan,C. Chen, Biosens.Bioelectron. 19 (2004)1635-1640.
4. C. Danielle, S. Michelle, A. Ivo,Z. Aldo, Chem. Mater.15[24](2003)4658-4665.
5. Y. Qiu,L. Gao, J. Phys. Chem. B. 109[42] (2005)19732-19740.
6. Q. L. Yang, J. Zhai, L. Feng, Y. L. Song, M. X. Wan, L. Jiang, W. G. Xu,Q. S. Li, Synth. Met.135 -136 (2003)819-820.
7. A. K. Giri, J. Appl. Phys.81 (1997)1348-1350.
8. A.K. Giri, and D. Chakravorty, *Trans. Ind. Ceram. Soc*.,50 (1991)28-32.
9. C.L. Chein, Science and technology of nanostructured magnetic materials, in:G.C. Hadjipanayis, G.A. Prinz (Eds.),Plenum Press, New York, 1991.
10. T. Ambrose, A. Gavrin,C. L. Chien, J. Magn. Magn.Mater.116 (1992)L311-L314.
11. S. Linderoth, M. S. Pedersen, J. Appl. Phys.75(1994) 5867-5869.
12. A. K. Giri, C. De Julian,J. M. Gonzalez, J. Appl. Phys.76 (1994)6573-6575.
13. M. Zhao, Y. Zhou, M. L. Bruening, D. E. Bergbreiter,R. M. Crooks, Langmuir.13 (1997)1388-1391.
14. Y. Park, Y. Ito,Y. Imanishi, Chem. Mater. 9[12](1997)2755-2758.
15. L. Li, J. Jiang,F. Xu, Eur. Polym. J.42[10] (2006)2221-2227.
16. J.L.Snoek, Physica. 14[4] (1948) 207–217.
17. T. Nakamura, T.Tsuoka, K.Hatakayama, J.Magn.Magn.Mater. 138[3](1994)319-328.
18. H. M. Xiao, X. M. Liu, S.Y. Fu, Compsites Science and Technology.66[13] (2006)2003-2008.
19. F. Sauzedde, A.E. Smissari,C. Pichot, J.Colloid.Polym.Sci.277(1999)846- 855.
20. L. Li, H. Qiu, H. Qian, B. Hao, X.Liang,J PhysChem C. 114[14] (2010)6712-6717.
21. N. Li, Y. Huang, F. Du, X. B. He, X. Lin, H. J. Gao, Y. F. Ma,F. F. Li, Y. S. Chen and P. C. Eklund, Nano Lett., 2006, 6, 1141.

*****